Article

# Improved Detection and Quantification of Cyclopropane Fatty Acids via Homonuclear Decoupling Double Irradiation NMR Methods

Dilek Eltemur, Peter Robatscher, Michael Oberhuber, and Alberto Ceccon*

Cite This: *ACS Omega* 2023, 8, 41835−41843

Read Online

ACCESS | Metrics & More | Article Recommendations | Supporting Information

**ABSTRACT:** Over the years, NMR spectroscopy has become a powerful analytical tool for the identification and quantification of a variety of natural compounds in a broad range of food matrices. Furthermore, NMR can be useful for characterizing food matrices in terms of quality and authenticity, also allowing for the identification of counterfeits. Although NMR requires minimal sample preparation, this technique suffers from low intrinsic sensitivity relative to complementary techniques; thus, the detection of adulterants or markers for authenticity at low concentrations remains challenging. Here, we present a strategy to overcome this limitation by the introduction of a simple band-selective homonuclear decoupling sequence that consists of double irradiation on ¹H during NMR signal acquisition. The utility of the proposed method is tested on dihydrosterculic acid (DHSA), one of the cyclopropane fatty acids (CPFAs) shown to be a powerful molecular marker for authentication of milk products. A quantitative description of how the proposed NMR scheme allows sensitivity enhancement yet accurate quantification of DHSA is provided.
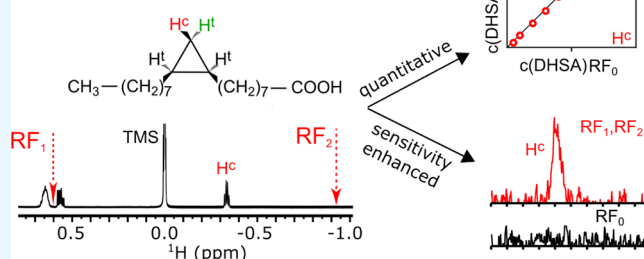
## ■ INTRODUCTION

Food quality and authentication are challenging topics that several analytical techniques are facing.[1−3] Over the years, an increasing number of consumers are getting more conscious about nutrition, quality, and origin of foods.[4,5] Therefore, a highly detailed characterization and content of unique markers to establish the quality and authenticity of foods is needed.[2,6] In recent years, Nuclear Magnetic Resonance (NMR) spectroscopy has established a significant role in the field of food science and technology and has become one of the most powerful analytical tools to identify organic substances as well as to elucidate their chemical structures in various food matrices.[7] Given its intrinsic nondestructive character, high reproducibility, and accuracy, NMR represents a compelling alternative to other analytical tools, such as GC-MS and LC-MS. Quantitative NMR (qNMR) spectroscopy-based analysis allows to determine the absolute content of specific markers since the measured area of the NMR signal is directly proportional to the number of observed nuclei (i.e., ¹H, ¹³C or ³¹P). In qNMR, the signal-to-noise ratio (SNR) and the choice of an appropriate standard (either internal, external, or electronic reference methods) play a crucial role in determining the accuracy and precision of the concentration measurements.[8−10] Despite all these advantages, NMR suffers from an inherently low sensitivity as a consequence of low spin polarization, which is governed by Boltzmann statistics at thermal equilibrium.[11] Although commonly confused with

sensitivity, the concept of SNR is preferred in the NMR community since it is considered well-defined and easy to measure for a specific signal on a given spectrum.[12] For example, SNR of a single-scan experiment acquired on ¹H nuclei (the most sensitive among NMR active nuclei) can be expressed as $SNR \sim \gamma_H^3 \times N \times B_o^2 \times D$, where $\gamma_H$ is the gyromagnetic ratio of ¹H, $N$ is the concentration of ¹H in the NMR sample, $B_o$ is the external applied magnetic field, and $D$ is an additional term that considers the sensitivity of the detector.[13] It clearly appears that for a given concentration $N$, SNR can be enhanced by (a) increasing the strength of static magnetic fields ($B_o$) and (b) reducing the noise in signal acquisition ($D$), i.e., cooling the wires of the detection coil by using cryogenic cold-NMR probes. Unfortunately, this strategy for sensitivity enhancements comes at a high cost and is not always achievable especially in small, medium−sized research groups. Additionally, recent NMR instrumentation advancements (higher magnetic fields or microcryoprobes technology)[14,15] and hyperpolarization techniques have shown great promise in enhancing NMR sensitivities by multiple orders of
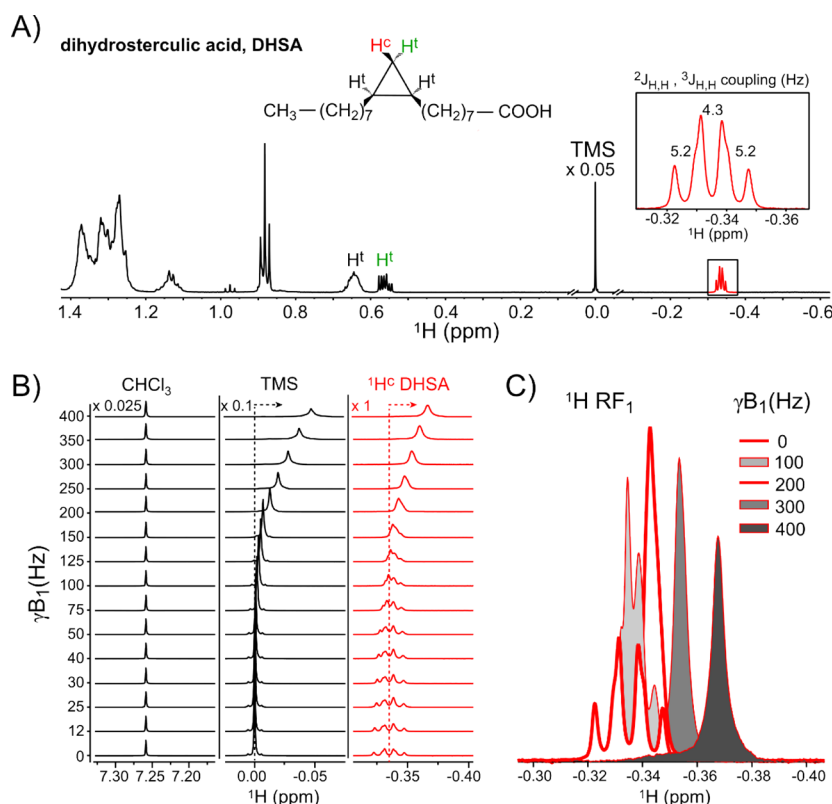
**Figure 1.** Effect of the single irradiation RF field (RF$_1$) on the signal intensity of the *cis*-methylene proton ($^1$H$^c$) in the cyclopropane ring of dihydrosterculic acid, DHSA. (A) $^1$H NMR spectrum of DHSA (CDCl$_3$, 600 MHz, 25 °C) in the region from −0.60 to 1.40 ppm and the chemical structure of DHSA with protons of the cyclopropane ring identified as cis and trans by the labels H$^c$ and H$^t$, respectively. The portion of the spectrum enclosed in the black box (and zoomed in in the upper right part) shows the characteristic quartet signal arising from coupling of $^1$H$^c$ to three $^1$H$^t$ in the cyclopropane ring and the corresponding coupling constants (in Hz). (B) Stacked $^1$H NMR spectra of CHCl$_3$ (black), TMS (black), and $^1$H$^c$ proton of DHSA (red) as a function of single RF field (RF$_1$) strengths. The arrows near the vertical dotted lines highlight the chemical shifts caused by the Bloch−Siegert effect. (C) Overlay of $^1$H$^c$ signals obtained at different RF field strengths. Note that signals from TMS and $^1$H$^c$ in parts B and C were referenced and scaled to the CHCl$_3$ signal, as described in the Experimental Section. All measurements were performed on a 0.60 mg mL$^{-1}$ (standard) DHSA sample.

magnitude. Thus, the need for additional specialized and expensive equipment may restrict the widespread application or adoption of these techniques, particularly in the field of food analysis. Other strategies to increase SNR, which include the use of paramagnetic agents to shorten the spin−lattice ($T_1$) relaxation time of the nucleus of interest, have been described.[16,17]

Here, we explore one of the most important (but surprisingly understudied) aspects of decoupling in NMR spectroscopy. Although signal decoupling can improve the resolution of overcrowded spectra due to the collapse of multiplet into singlet, the former has the important benefit of increasing SNR. Here, we provide a quantitative description of how the introduction of a simple decoupling scheme not only results in an increased SNR on $^1$H 1D NMR experiments but also allows an accurate quantification of the analyte. We tested our method on the detection and quantification of dihydrosterculic acid (DHSA), as one of cyclopropane fatty acids (CPFAs) that has been identified as powerful molecular marker in establishing the authenticity of Protected Denomination of Origin (PDO) cheeses such as Parmigiano Reggiano.[18−22] Hence, the CPFA methodology on the authentication of Hay Milk is a current interest as its specification of production prohibits the use of silage on cows feeding.[23] Briefly, CPFAs, mainly lactobacillic and dihydrosterculic acids, are uncommon fatty acids containing

a three-carbon ring located at different positions of the fatty acid chain (Figure 1A). They are known to be components of bacterial membranes in both Gram-positive and Gram-negative as a response to stress conditions.[24] So far, CPFAs have been identified in a wide variety of animal-derived foods (i.e., dairy and meat products) and their presence correlate with the presence of maize silage in the forage used in livestock farming.[23] Recently, the presence of CPFAs in milk and dairy products has been linked to the field of food authentication; in fact, products such as Parmigiano Reggiano cheese (PDO) and Hay Milk, where the usage of silage is forbidden (EU 1151/12, EU 2016/304), should be free of any CPFAs.[25] Consequently, given the high commercial values of the latter products and the rise of food fraud, CPFAs are considered molecular and quality markers in dairy products.[22,26] Furthermore, since the potential role and effects of CPFAs on human health remain elusive as well as their effects in human metabolism, the development of different analytical methods to improve their correct and accurate detection and quantification is required.

## ■ EXPERIMENTAL SECTION

**Materials.** All-*cis*-methyleneoctadecanoic acid (DHSA) (microbial cyclopropane fatty acid, Cas no. 5711-28-4, neat purity 98%, Abcam, Cambridge, UK) and deuterated chloroform (CDCl$_3$, 0.03 vol/vol % TMS as an internal standard, Cas no. 865-49-6, >98% D, Sigma-Aldrich, Saint Louis, Missouri,

USA) were used. All other used chemicals (solvents, standards, and reagents) were of analytical grade.

**NMR Sample Preparation.** A DHSA standard stock solution was prepared by dissolving 3.00 mg of DHSA in 5.00 mL of $CDCl_3$ (containing 0.03 vol/vol % TMS as an internal standard) to reach a concentration of 0.60 mg mL$^{-1}$.

*Standard solutions* of DHSA were prepared by diluting the stock solution with $CDCl_3$ to the desired concentrations of DHSA in the range from 0.60 to 0.0001 mg mL$^{-1}$.

*Complex mixtures* of DHSA were obtained by dissolving 50.00 mg of freeze-dried hay milk sample (free of DHSA) in 1.00 mL of $CDCl_3$ containing the desired concentration of DHSA. The mixture was then vortexed for 1 min at room temperature and centrifuged at maximum speed (12,000 rpm) for 30 min at 4 °C to remove any insoluble particles that could affect the NMR shim during measurements. 800 $\mu$L of the supernatant was then transferred into an NMR tube for the $^1$H NMR analysis. Authenticity of the lyophilized hay milk sample (in terms of the absence of any DHSA) was confirmed by GC-MS and $^1$H NMR analyses. To avoid evaporation of $CDCl_3$ during sample preparation and NMR analysis (that could affect a correct quantification of DHSA), the DHSA stock solution and the NMR tubes in the autosampler were kept at 4 °C prior to preparation of the NMR samples and analysis, respectively. A list of concentrations for all DHSA samples (standard solutions and complex mixtures) used in the current study is available in Table S1.

**NMR Spectroscopy.** All NMR experiments were carried out at 25 °C using a 600 MHz spectrometer (JNM-ECZ from JEOL Ltd., Tokyo, Japan), equipped with a room-temperature "Royal" HFX/FGSQ probe and an autosampler cooled at 4 °C. All NMR data were processed and analyzed with Delta NMR Data Processing software (JEOL Ltd., Tokyo, Japan).

**Determination of Spin−Lattice Relaxation Time ($T_1$) of DHSA Protons.** Values of $T_1$ for protons in the terminal methyl group and in the methylene groups of the fatty acid chain and the *cis*-methylene proton in the cyclopropane ring of the DHSA molecule (see Figure 1) were obtained from a simple 180° $\tau$ (repetition time) $\tau$ 90° inversion recovery pulse sequence experiment ("double pulse" in the JEOL Ltd. pulse sequence library) acquired on a 0.60 mg mL$^{-1}$ DHSA standard sample in $CDCl_3$. A set of 32 spectra were recorded with an array of $\tau$ delays (varying from 10 ms to 20 s) and a relaxation delay of 40 s, enough to reach thermal equilibrium. $T_1$ values were obtained from the following equations:

$$M_z(\tau) = M_z^0[1 - 2\exp^{(-\frac{\tau}{T_1})}] \quad (1)$$

where $M_z^0$ is the initial $z$- magnetization and $\tau$ is the repetition time. A list of $T_1$ values for all previously listed protons of the DHSA molecule is provided in Table S2.

**Acquisition and Processing of $^1$H NMR Spectra.** All 1D $^1$H NMR experiments were performed using a slight in-house modification of the pulse sequence "qnmr_experiment" (JEOL Ltd.), with the introduction of $^{13}$C decoupling during signal acquisition to achieve elimination of $^{13}$C-satellite signals of TMS and analytes. Complete removal of interfering $^{13}$C-satellite has been shown to improve the accuracy in the quantification of the NMR signals.[27] $^{13}$C decoupling was achieved by a multipulse, ultrabroad bandwidths decoupling sequence, namely, MPF-8.[28] All samples were analyzed in triplicate at 25 °C with the following acquisition parameters: acquisition time (AQ) = 4 s, spectrum width (SW) = 13 ppm

(with filter limit = 4), frequency offset = 3 ppm, 90° $^1$H pulse = 7.9 $\mu$s, receiver gain = 56, dummy scans = 4, number of scans (NS) for each experiment see Table S1, and relaxation delay of 20 s. Note that (a) at a given DHSA concentration, the same NS were used for acquisition of 1D $^1$H NMR spectra with or without homonuclear decoupling and (b) the value for relaxation delay is >5 times longer than the $T_1$ value for the slowest relaxing terminal methyl protons ($T_1$ values determined as described above and reported in Table S2), therefore allowing complete relaxation between two pulses.

Homonuclear decoupling of the *cis*-methylene proton of DHSA was achieved by introducing a selective RF field ($^1$H RF$_1$) at $\delta_1$ = 0.60 ppm during acquisition time. The second "dummy" RF field ($^1$H RF$_2$) was applied at $\Delta\delta_2 = \delta_{H^c} - \delta_1 = -0.94$ ppm, where $\delta_{H^c}$ (−0.34 ppm) is the chemical shift of the *cis*-methylene proton in the cyclopropane ring. In all experiments where both RF fields ($^1$H RF$_1$ and $^1$H RF$_2$) were applied, the RF field strength of $^1$H RF$_2$ was set to the same values as those of $^1$H RF$_1$. A list of the RF field strengths (and corresponding attenuations) used in the current study is available in Table S3.

For processing of all 1D $^1$H NMR spectra, an exponential window function was employed with a line broadening factor of 0.3 Hz and zero-filled to 48,000 points prior to Fourier transformation. Each spectrum was then manually phase-corrected and baseline-corrected. Note that all chemical shifts were calibrated relative to the chemical shift of the chloroform peak (7.26 ppm for $^1$H NMR) and not to the chemical shift of TMS.

**Quantification of DHSA in Standard Solution and Complex Mixture.** Quantitative analysis of DHSA in standard solution and in complex mixture was obtained by integrating the peak area corresponding to the signal of the *cis*-methylene proton (centered at ∼−0.34 ppm) using the methyl signal of TMS as the internal standard. In all experiments, the integral limits (−0.31 ppm < Int < −0.35 ppm) were used for quantifying the signal of the *cis*-methylene proton independently of the pulse sequence implemented (i.e., with or without homonuclear decoupling). Note that in all experiments, $^{13}$C-satellite signals were absent due to the introduction of $^{13}$C decoupling during signal acquisition as described above. Experimental concentrations of DHSA, $c(\text{DHSA})_{\text{exp}}$, expressed as mg mL$^{-1}$ were calculated as follows:

$$c(\text{DHSA})_{\text{exp}} = \text{MW}_{\text{DHSA}} \times \frac{A_{\text{DHSA}}}{A_{\text{TMS}}} \times \frac{N_{\text{TMS}}}{N_{\text{DHSA}}} \times \frac{c(\text{TMS})}{\text{MW}_{\text{TMS}}}$$

$$(2)$$

where $\text{MW}_{\text{DHSA}}$ and $\text{MW}_{\text{TMS}}$ are the molecular weight of DHSA (296.49 g mol$^{-1}$) and TMS (88.22 g mol$^{-1}$), respectively; $A$ and $N$ are the integrated area and number of $^1$H of DHSA and TMS, respectively. $c(\text{TMS})$ is the concentration of TMS (expressed as mg mL$^{-1}$) in the NMR tube.

**Signal-to-Noise Ratio (SNR), Limit of Detection (LOD), and Limit of Quantification (LOQ) of DHSA.** For each 1D $^1$H NMR spectrum, the corresponding SNR was calculated by using the S/N tool implemented on Delta Software (JEOL Ltd.). The NMR signal and noise were extracted in the range of −0.29/−0.39 ppm and −0.45/−0.65 ppm, respectively, from 1D $^1$H spectra measured on both DHSA standard and complex mixture samples. The LOD of the DHSA signal was determined empirically through a visual evaluation. Specifi-
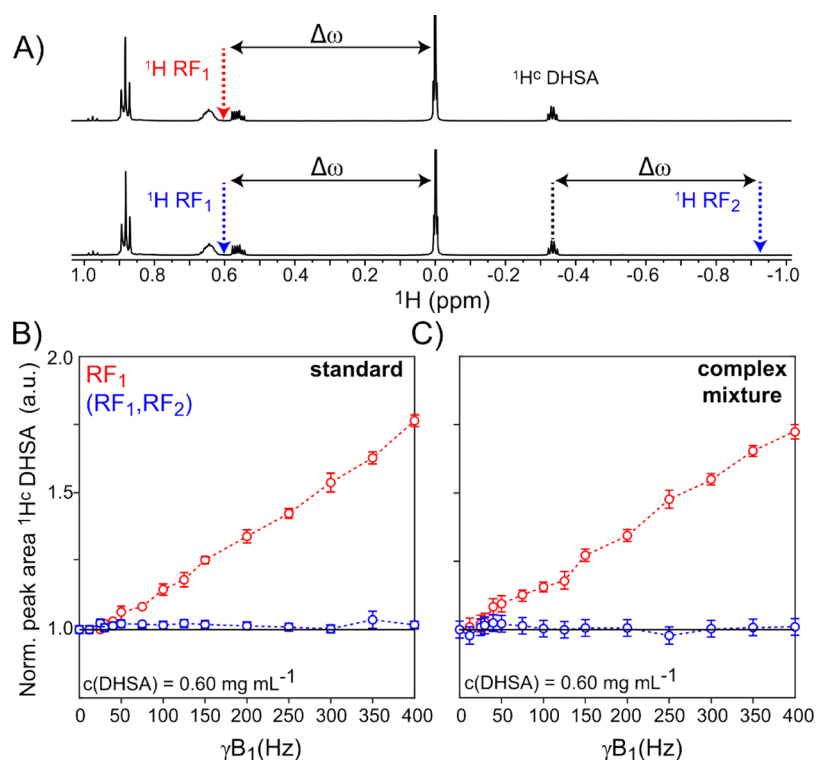
**Figure 2.** Effect of homonuclear decoupling on the quantification of the DHSA molecule. (A) Region of the $^1H$ NMR spectrum of DHSA (CDCl$_3$, 600 MHz, 25 °C) showing the offset of the applied single (RF$_1$, top panel) and double (RF$_1$, RF$_2$, bottom panel) selective RF fields, with $\omega^{RF_1}$ and $\omega^{RF_2}$ values equal to 0.60 and −0.97 ppm, respectively. Plots of integrated $^1H^c$ DHSA peak areas (referenced to TMS signal) as a function of the applied RF field strengths are shown for (B) "standard" solution (containing only DHSA) and (C) in a complex mixture (DHSA spiked to freeze-dried milk as described in the Experimental Section). Changes in signal areas employing single (RF$_1$) and double (RF$_1$, RF$_2$) selective frequencies are colored red and blue, respectively. All $^1H^c$ DHSA peak areas shown in the plots are normalized to the peak area measured for $\gamma B_1 = 0$ Hz.

cally, it was determined when the shape of the signal originating from the *cis*-methylene proton of the cyclopropane ring in DHSA could be visually identified at the correct chemical shift (approximately −0.34 ppm). This corresponds to SNR ~2−3. On the contrary, the LOQ of DHSA was set for SNR ≥ 10, allowing the concentration of DHSA to be uniquely defined and in agreement with previous studies.[29−31] A list of observed SNR for different concentrations of DHSA in standard solution and in complex mixtures is provided in Table S4.

## ■ RESULTS AND DISCUSSION

The 1D $^1H$ NMR spectrum in the region from −0.60 to 1.40 ppm of a DHSA standard solution is shown in Figure 1A (the full spectrum is available in Figure S1). Following the assignment of the chemical shift performed by Knothe, protons in the cyclopropane rings show distinct chemical shifts.[32] The upfield peak at ~−0.33 ppm can be attributed to the *cis*-methylene proton, $^1H^c$ (labeled in red in Figure 1) while downfield peaks at ~0.55 and ~0.64 ppm can be assigned to the *trans*-methylene proton, $^1H^t$ (labeled in green in Figure 1), and to the two *trans*-methine protons, $^1H^t$ (labeled in black in Figure 1), of the cyclopropane ring, respectively. The downfield signals at ~0.88 and ~1.25 ppm, which can be assigned to the methylene and methyl protons of the fatty acid chain of DHSA, respectively, were only included in the study for the determination of their $T_1$ values (see Experimental Section and Table S2).

Among all observable signals of DHSA, the upfield-shifted resonance of the *cis*-methylene proton in the cyclopropane ring

(H$^c$, see Figure 1A) is generally picked as the target signal for quantification of DHSA, given its distinct chemical shift far from any other resonances even in complex mixtures.[22,32] Additionally, homonuclear spin−spin coupling of the *cis*-methylene proton with its geminal *trans*-methylene proton ($^2J_{H,H}$ ~ 5 Hz) and with the two vicinal *trans*-methine protons ($^3J_{H,H}$ ~ 4 Hz) of the cyclopropane ring gives rise to the multiplicity pattern of the upfield signal (Figure 1, inset), where the size of the splitting (expressed through the coupling constant, $J$ in Hz) corresponds to the energy difference of the coupling partners, i.e., the spin arrangement ($\alpha$ or $\beta$ state) of the protons in the adjacent group.

Although $J$-coupling constants are useful NMR parameters that provide structural information, a correct quantification of organic molecules can also be affected by signal broadening, which also occurs due to $^1H - ^1H$ spin couplings. Given the distinct chemical shift of the *cis*-methylene proton, the observed $J$-splitting of this proton is highly undesirable in this case since it significantly affects the sensitivity (expressed as SNR; see Table S4) in the accurate quantification of DHSA.

Homonuclear spin−spin coupling of *cis*-methylene proton with its neighboring proton spins can be easily removed by applying a single selective radiofrequency (RF$_1$) field on $^1H$ at 0.60 ppm, with a pulse bandwidth covering both geminal *cis*-methylene and vicinal *trans*-methine protons of the cyclopropane ring of DHSA (Figure 1A).

By employing an array of different RF field strengths, $\gamma B_1$, (shown in Figure 1B), we found that a selective pulse with $\gamma B_1$ ~ 200 Hz allows complete decoupling of *cis*-methylene proton into a singlet and results in an increase in the signal intensity of
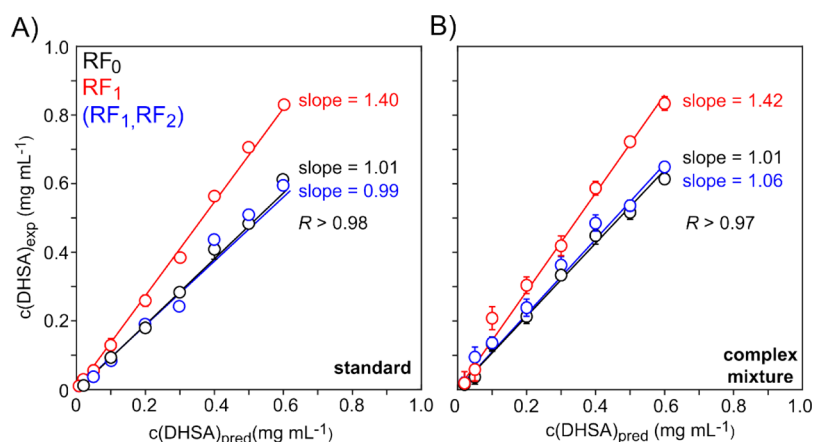
**Figure 3.** Correlation plots comparing predicted (pred) and experimental (exp) DHSA concentrations determined from the integrated area of the *cis*-methylene proton signal of the cyclopropane ring in $^1$H NMR spectra. Concentrations of DHSA recast from NMR experiments acquired with single ($RF_1$) and double ($RF_1$, $RF_2$) selective decoupling pulses are colored red and blue, respectively. Concentrations of DHSA obtained from reference experiments without decoupling ($RF_0$) are labeled in black. Measurements were performed on (A) "standard" solution (with only DHSA) and (B) in "complex mixture" (with DHSA dissolved in milk extract as described in the Experimental Section). Slopes and Pearson correlation coefficients ($R$) are reported in the figures. Measures were performed in triplicate, and error bars are reported in the plots.

this proton, which is shown in Figure 1C. While experiments performed with $\gamma B_1 < 200$ Hz led to incomplete decoupling, stronger RF field strengths ($\gamma B_1 \geq 200$ Hz) induce Bloch−Siegert (BS) shifts on the signal of *cis*-methylene proton ($\Delta\omega_{BS}^{H^c}$ = 10 ppb for $\gamma B_1 = 200$ Hz). Thus, excessive RF field strengths ($\gamma B_1 > 300$ Hz) causes phase distortion, massive shifts and signal broadening (Figure 1B, upper part).[33]

Unusually, the position of the TMS signal in the 1D $^1$H DHSA spectrum is between the chemical shift of the applied single selective radiofrequency ($RF_1$) and the *cis*-methylene proton, at 0.60 and $\sim-0.34$ ppm, respectively, with $\omega^{H^c} < \omega^{TMS} < \omega^{RF_1}$. It follows that the signal corresponding to TMS (Figure 1B, mid panel) is also affected by the BS effect induced by the decoupling frequency, resulting in an upfield shift ($\Delta\omega_{BS}^{TMS} = -10.4$ ppb for $\gamma B_1 = 200$ Hz) as well as strong broadening of the signal. Since quantification of molecules with NMR requires the integration of reference signal (TMS in our case), we wondered whether under this condition any quantitative analysis of DHSA is therefore precluded.

Thus, we monitored the changes in $^1$H$^c$ DHSA signal area as a function of the RF field strength ($0 \leq \gamma B_1 \leq 400$ Hz) by employing a single ($RF_1$) selective RF field (as depicted in Figure 2A, top panel). In Figure 2B,C, the normalized integrated signal of $^1$H$^c$ DHSA ($nA_{DHSA}^{i\,Hz}$) as a function of the decoupling field strength is calculated as follows:

$$nA_{DHSA}^{i\,Hz} = \frac{A_{DHSA}^{i\,Hz} * A_{TMS}^{0\,Hz}}{A_{TMS}^{i\,Hz} * A_{DHSA}^{0\,Hz}} \qquad (3)$$

where $A_{DHSA}^{i\,Hz}$ and $A_{TMS}^{i\,Hz}$ are peak areas corresponding to $^1$H$^c$ DHSA and TMS signals, respectively, measured at $\gamma B_1 = i$ Hz (with $0$ Hz $< i \leq 400$ Hz). $A_{DHSA}^{0\,Hz}$ and $A_{TMS}^{0\,Hz}$ are peak areas corresponding to $^1$H$^c$ DHSA and TMS signals, respectively, measured at $\gamma B_1 = 0$ Hz. Measurements were performed on sample containing 0.60 mg mL$^{-1}$ of DHSA standard dissolved in CDCl$_3$ (labeled as "standard" in Figure 2B) as well as on spiked samples (labeled as "complex mixture" in Figure 2C) where DHSA was added to freeze-dried milk powder dissolved in CDCl$_3$ as described in Experimental Section. The latter experiment was performed to test the validity of our method in

complex environments and to check for any matrix effect. As expected, the same chemical shifts were observed in $^1$H spectra for *cis*- and *trans*- protons of the cyclopropane ring of DHSA in standard and complex mixture (Figure S1).

Since all RF-strength-dependent experiments were acquired on NMR samples with the same amount of DHSA, we did not expect any significant variation in the value of $nA_{DHSA}^{i\,Hz}$ as a function of the applied $i$ decoupling field. The value of $nA_{DHSA}^{i\,Hz}$ (shown as red circles in Figure 2B,C) increases progressively, reaching almost 180% of the initial value at the maximum applied $\gamma B_1$ value (= 400 Hz). The resulting linear increase in $nA_{DHSA}^{i\,Hz}$ values in the plot can be attributed directly to the BS effect on the TMS signal described above. In fact, broadening of the TMS signal reduces the denominator in eq 3 causing an increase in the value of $nA_{DHSA}^{i\,Hz}$.

Therefore, quantification of DHSA is not amenable under such decoupling conditions: for $\gamma B_1 = 200$ Hz, the field strength required for a complete decoupling of *cis*-methylene proton, the increase of the normalized integrated signal of $^1$H$^c$ DHSA ($\Delta nA_{DHSA}^{200\,Hz}$) corresponds to $\sim40\%$ making quantification of DHSA extremely inaccurate under these specific conditions. To overcome this issue, we exploited the homonuclear decoupling sequence recently proposed by Saito and co-workers.[34] Shortly, the method requires, together with the decoupling selective RF field ($RF_1$), the addition of a second "dummy" selective RF field ($RF_2$) performed upfield to the signal of interest to decouple (in our case the *cis*-methylene proton (Figure 2A, lower panel)). More specifically, the following conditions must be fulfilled: (a) the differences in chemical shifts ($\Delta\omega$) between the applied first selective radiofrequency ($RF_1$) and the TMS signal and between the signal of the second selective radiofrequency ($RF_2$) and the proton(s) of interest are equal, and (b) the applied radiofrequency strength for $RF_1$ and $RF_2$ is the same.

The resulting normalized signal of $^1$H$^c$ DHSA ($nA_{DHSA}^{i\,Hz}$) as a function of the decoupling field strength applying both $RF_1$ and $RF_2$, is shown in Figure 2B,C. The addition of the second selective RF field ($RF_2$) prevents any increase in the value of $nA_{DHSA}^{i\,Hz}$ as a function of RF strength. This is a direct consequence of the fact that broadening of the TMS signal caused by $RF_1$ equals the broadening of the signal of the *cis*-

methylene proton caused by $RF_2$, thus preserving a constant value of $nA_{DHSA}^{i\,Hz}$ at different decoupling field strengths.

The effectiveness of the proposed NMR method was tested via the quantification of DHSA over a series of "standard" NMR samples where the (pure) DHSA stock solution (predicted concentration, $c(DHSA)_{pred}$, = 0.60 mg mL$^{-1}$) was progressively diluted with $CDCl_3$ to $c(DHSA)_{pred}$ = 0.0001 mg mL$^{-1}$ (see Table S1 for the list of concentrations). As for Figure 2, measurements were also performed in complex mixtures where different amounts of DHSA were spiked to freeze-dried milk resuspended in $CDCl_3$ (see Experimental Section for details).

Note that the LOQ of DHSA in both standard and complex mixtures was set for SNR values ≥10; therefore, quantification of DHSA below ~0.01 mg mL$^{-1}$ was not yet achievable under these experimental conditions. Figure 3 shows correlation plots comparing $c(DHSA)_{pred}$ and experimental concentrations of DHSA, $c(DHSA)_{exp}$, calculated from the integrated intensity of the *cis*-methylene proton signal in $^1H$ NMR spectra, referenced to the signal of TMS as described in the Experimental Section.

As expected, linear correlation (Figure 3, black line) exists between $c(DHSA)_{pred}$ and $c(DHSA)_{exp}$ obtained from $^1H$ NMR spectra where the signal of the *cis*-methylene proton was not decoupled (no RF applied). However, experimental concentrations, $c(DHSA)_{exp}$, calculated from the signal of *cis*-methylene proton decoupled with a single selective field ($RF_1$) at $\gamma B_1$ = 200 Hz were overestimated by ~40% in the standard solution and ~42% in the complex mixture, respectively, as shown in Figure 3 (red line). It is straightforward to show from eq 3 that overestimation in $c(DHSA)_{exp}$ is equal (within the experimental error) to the $\Delta nA_{DHSA}^{200\,Hz}$ value, as described above. Nonetheless, when both $RF_1$ and $RF_2$ are applied during signal acquisition, $c(DHSA)_{exp}$ values are linearly correlated to $c(DHSA)_{pred}$ with slope ~1 (Figure 2, blue line), thus confirming that a correct and accurate quantification of DHSA achieved from the decoupled *cis*-methylene proton signal requires the presence of both ($RF_1$, $RF_2$) selective pulses.

Given the intrinsic low concentration of DHSA in milk samples (as low as 2.5 $\mu$g mL$^{-1}$)[22] from cows fed with the addition of maize silage, improving the SNR is an essential requirement for accurate integration of the NMR signal and, therefore, detection and/or quantification of the analyte. After solving the issue of quantification from the decoupled *cis*-methylene proton signal of DHSA, we focused on providing a quantitative analysis of SNR calculated from NMR experiments in the presence of decoupling field(s). As previously shown in Figure 1C, collapsing the DHSA signal quartet into a singlet improves the sensitivity of the DHSA signal. A quick comparison of peak heights estimated from the *cis*-methylene proton of DHSA in the presence ($\gamma B_1$ = 200 Hz) and absence of a single decoupling field ($RF_1$) shows a ~2.2-fold increase in intensity (Figure 1C, red traces).

Nonetheless, a more rigorous analysis where SNR of the DHSA was estimated from decoupled NMR experiments acquired with single ($RF_1$) or double ($RF_1$, $RF_2$) selective pulses is described here. Signal of DHSA and spectral noise were extracted in the range of −0.29/−0.39 and −0.45/−0.65 ppm (Figure 1A and Experimental Section for details), respectively, from a series of $^1H$ spectra acquired over the same set of DHSA concentrations, as indicated in Figure 3 and in Table S1.

Figure 4 plots the ratio $R$ of the experimental $SNR_{RFi\,(with\,i=1\,or\,1,2)}$, obtained from $^1H$ spectra acquired in
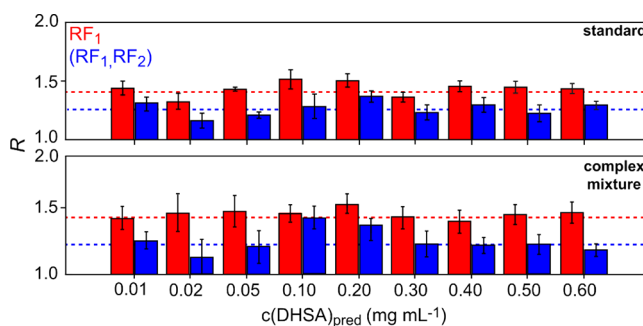


**Figure 4.** Bar graph of the experimental ratios $R$ (= $SNR_{RF_i}/SNR_{RF_0}$, with $i$ = 1 or 1,2) measured on the *cis*-methylene proton signal of the cyclopropane ring in DHSA as a function of the concentration of DHSA in standard solution (upper panel) and in complex mixture (freeze-dried milk spiked with DHSA, lower panel). $Rs$ values obtained from decoupled NMR experiments acquired with single ($RF_1$) and double ($RF_1$, $RF_2$) selective pulses are shown as red and blue bars, respectively. Red and blue dotted lines in both panels indicate the average $SNR_{RF}/SNR_{RF_0}$ values, respectively. NMR signal and noise were extracted as described in the Experimental Section. NMR analyses were carried out in triplicate for each experiment.

the presence of $RF_1$ (red bars) or $RF_1$, $RF_2$ (blue bars), to $SNR_{RF_0}$ measured on refence $^1H$ spectra without applying any decoupling field. Note that plotting of the normalized $Rs$ as a function of concentrations of DHSA allows direct comparison between experiments acquired with different numbers of scans (listed in Table S1), provided that at a given concentration $i$ of DHSA, values of $SNR_{RFi\,(with\,i=1\,or\,1,2)}$ and $SNR_{RF_0}$ are extracted from $^1H$ spectra obtained with the same number of scans.

Average values of $R$ obtained for 1D $^1H$ NMR spectra acquired in the presence of $RF_1$ (red bars) or $RF_1$, $RF_2$ (blue bars) cluster around ~1.4 ($\pm$0.1) and ~1.2 ($\pm$0.1), respectively (Figure 4). No significant differences in $R$ values were observed among experiments performed on DHSA in "standard" and in "complex mixture", showing the absence of any matrix effect.

Values of $R$ are systematically higher than 1, indicating an overall increase of the SNR attributed to the *cis*-methylene proton signal of DHSA on decoupled experiments, regardless of the number of applied RF fields. Note that the variability on $R$ values as a function of the concentration of DHSA (although within the experimental error calculated from triplicate) can be attributed to spectral artifacts during NMR signal acquisition (i.e., distortion, shim). Interestingly, values of $R$ obtained in the presence of both $RF_1$ and $RF_2$ are lower than the ones obtained with only $RF_1$ by a factor of ~0.85. This loss in sensitivity can be attributed to the introduction of a second selective $^1H$ decoupling pulse ($RF_2$), which is applied simultaneously with $RF_1$ on the NMR probe, thereby requiring a more complicated time-share mode during signal acquisition that can partially affect sensitivity.[35,36]

Comparison of $Rs$ (shown in Figure 4) were performed under the conditions where $SNR^i$ ≥ 10 with $i \in \{RF_0, RF_1, RF_2\}$, thus above LOQ. Conversely, in the limit where SNR < 10 for at least one of experiments performed with and without decoupling, we decided to test "qualitatively" (by visual inspection of the NMR signal) whether decoupling of the
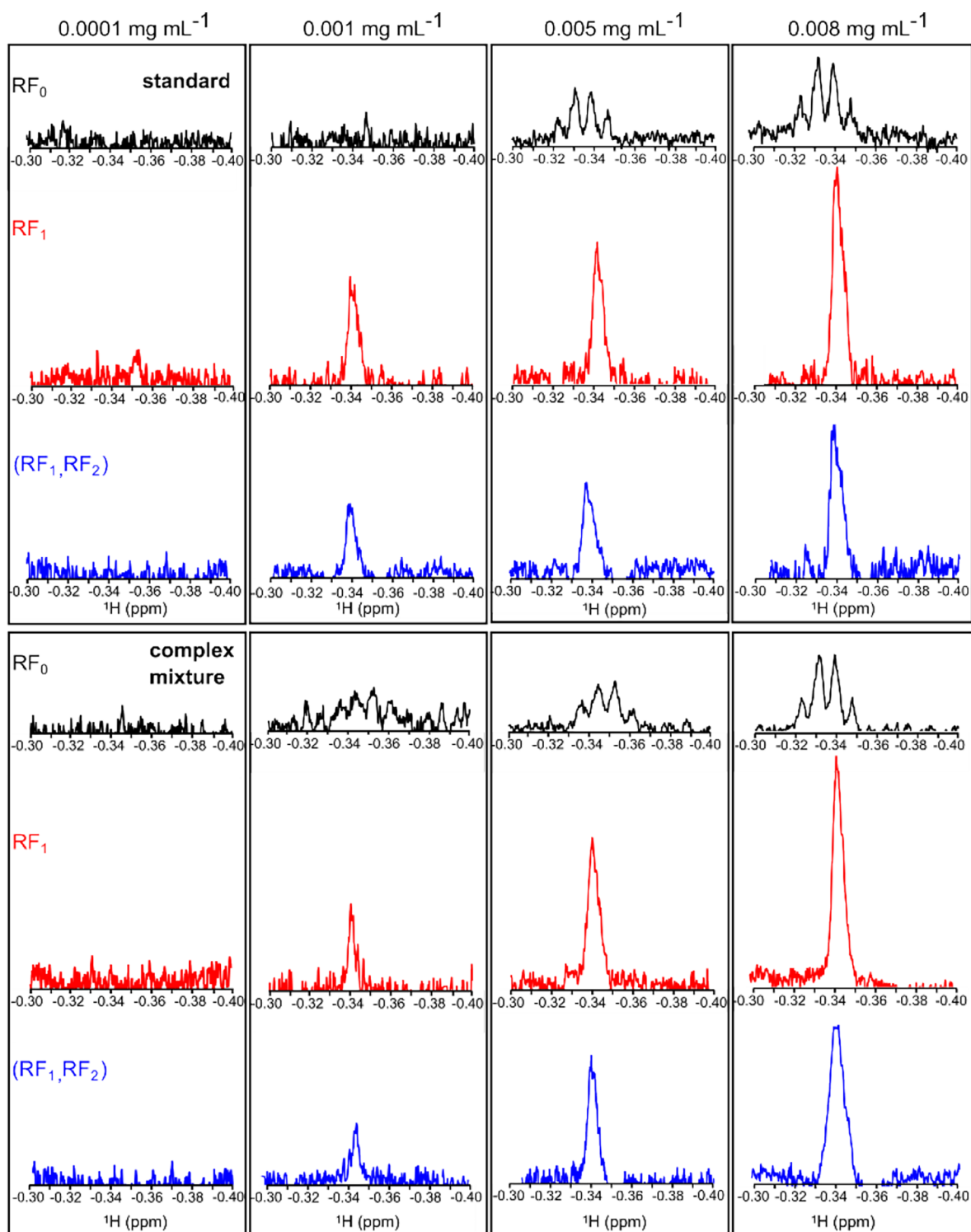
**Figure 5.** Improved detection of *cis*-methylene proton, $^1H^c$ signal from DHSA by employing single ($RF_1$) and double ($RF_1$, $RF_2$) selective pulses. NMR experiments acquired on four different concentrations of DHSA (0.0001, 0.001, 0.005, and 0.008 mg mL$^{-1}$) without decoupling ($RF_0$), with a single ($RF_1$) selective decoupling pulse and with the double-pulse ($RF_1$, $RF_2$) scheme are shown in black, red, and blue, respectively. Data obtained for the DHSA standard solution and in complex mixture are shown in the upper and lower panel, respectively. Correct comparison of DHSA signal intensities was achieved by using the CHCl$_3$ signal as reference, as described in the Experimental Section.

*cis*-methylene proton NMR signal can enhance sensitivity, defined as the ability to detect weak peaks close to the noise level.

As an example, NMR spectra measured for $c(DHSA)_{pred}$ at 0.0001, 0.001, 0.005, and 0.008 mg mL$^{-1}$ are shown in Figure 5: the top panels display $^1H$ spectra measured on DHSA standard, while the bottom panels display $^1H$ spectra acquired on DHSA in complex mixture. Reference spectra acquired without decoupling (Figure 5, no RF, in black) are compared with spectra where the collapsing of the *cis*-methylene proton signal into a singlet was achieved by applying a single $RF_1$ field with $\gamma B_1 = 200$ Hz (Figure 5, $RF_1$, in red). Note that correct

quantification of DHSA at these concentrations is in any case extremely error-prone (SNR $\sim$ 10); therefore, the above-described method where the second selective pulse ($RF_2$) is introduced during signal acquisition is beyond the scope. Furthermore, from the comparison of SNR measured on $^1H$ spectra with introduction of single and double RF fields (Figure 4 and as above-described), homonuclear decoupling achieved with a single RF field allows a better SNR, $\langle SNR^{RF_1} \rangle$ $\sim$ 1.2 $\langle SNR^{RF_1,RF_2} \rangle$.

For the two highest concentrations of DHSA shown in Figure 5 (0.005 and 0.008 mg mL$^{-1}$), the signal of a *cis*-methylene proton can be detected in the presence and in the absence of the single $RF_1$ decoupling field. However, a $\sim$2.0-fold increase in peak intensity and a $\sim$1.2-fold increase in SNR are gained for the $^1H$ spectrum acquired with a single decoupling field ($RF_1$), consistent with what observed for $c(DHSA)_{pred}$ = 0.60 mg mL$^{-1}$ (Figure 1C).

More impressive is how the detection of DHSA can be improved in the presence of $RF_1$ for $c(DHSA)_{pred}$ = 0.001 mg mL$^{-1}$, the second-lowest concentration of DHSA used in this study. While identification of the signal of *cis*-methylene proton on not-decoupled experiments is not possible ( $\langle SNR^{RF_0} \rangle$ < 2, therefore below LOD), the introduction of $RF_1$ increases sensitivity and allows detection of DHSA ( $\langle SNR^{RF_1} \rangle$ $\sim$ 8).

Under our experimental conditions, we found that detection of DHSA is precluded for $c(DHSA)_{pred} \leq$ 0.0001 mg mL$^{-1}$ regardless of any decoupling scheme.

## CONCLUSIONS

CPFAs are a class of secondary fatty acids that include DHSA, the most abundant CPFAs recently detected in milk and dairy products obtained from cows fed with maize silage. Given its importance as a molecular marker for authentication of high-value dairy products (i.e., Hay Milk, PDO-labeled cheeses), implementation of more accurate and precise approaches for the detection and quantification of DHSA is required. Although NMR spectroscopy is an important tool for monitoring food authenticity through the identification of specific markers, this methodology applied under standard conditions suffers from low sensitivity.

Here, we have quantitatively shown how the introduction of a simple and straightforward homonuclear decoupling scheme on $^1H$ NMR experiments, where a single radiofrequency, $RF_1$, field is applied during acquisition, can enhance both SNR and the detection sensitivity of DHSA. However, giving the peculiar chemical shift of *cis*-methylene proton, the $^1H^c$ signal from DHSA (upfield to the TMS signal), addition of a second "dummy" RF field ($RF_2$) is required to correctly quantify DHSA. The proposed method retains the option of using TMS as an internal standard for quantification, thus accounting for variations in instrument performance or sample conditions.

Previous NMR studies on CPFAs report LOD values of $\sim$0.0025 mg mL$^{-1}$ (SNR = 4) for DHSA standard solution.[22] Under similar experimental conditions and by employing homonuclear decoupling, we were able to detect DHSA signals down to a concentration of $\sim$0.001 mg mL$^{-1}$ (SNR = 8), indeed increasing the sensitivity by threefold. Thus, the gain in the detection sensitivity and SNR described in this study clearly shows the effectiveness of the proposed methodology in the detection and quantification of such specific molecular markers found at low concentrations in dairy products obtained with ensiled feeds. Given the increasing usage of NMR for the identification of counterfeits, developing novel NMR methodologies, boosting existing ones, and eventually combining data from different platforms (NMR and other techniques) represents an essential strategy to improve targeted identification of specific markers of adulteration in food science.

## ASSOCIATED CONTENT

### Supporting Information

The Supporting Information is available free of charge at https://pubs.acs.org/doi/10.1021/acsomega.3c06538.

Additional 1D $^1H$ NMR spectra of DHSA; the list of DHSA concentrations used throughout the study; NMR parameters; and full list of the estimated SNR values (PDF)

## AUTHOR INFORMATION

### Corresponding Author

**Alberto Ceccon** − *Laimburg Research Centre, Auer (Ora), BZ 39040, Italy;* orcid.org/0000-0002-2808-7262; Email: alberto.ceccon@laimburg.it

### Authors

**Dilek Eltemur** − *Laimburg Research Centre, Auer (Ora), BZ 39040, Italy; Faculty of Agricultural, Environmental and Food Sciences, Free University of Bozen-Bolzano, Bozen-Bolzano 39100, Italy*

**Peter Robatscher** − *Laimburg Research Centre, Auer (Ora), BZ 39040, Italy*

**Michael Oberhuber** − *Laimburg Research Centre, Auer (Ora), BZ 39040, Italy;* orcid.org/0000-0002-9989-7297

Complete contact information is available at:
https://pubs.acs.org/10.1021/acsomega.3c06538

### Author Contributions

The manuscript was written through contributions of all authors. All authors have given approval to the final version of the manuscript.

### Notes

The authors declare no competing financial interest.

## ACKNOWLEDGMENTS

## REFERENCES

(1) Ortea, I.; O'Connor, G.; Maquet, A. Review on Proteomics for Food Authentication. *J. Proteomics* **2016**, *147*, 212−225.

(2) Sobolev, A. P.; Thomas, F.; Donarski, J.; Ingallina, C.; Circi, S.; Cesare Marincola, F.; Capitani, D.; Mannina, L. Use of NMR Applications to Tackle Future Food Fraud Issues. *Trends Food Sci. Technol.* **2019**, *91*, 347−353.

(3) Lytou, A. E.; Panagou, E. Z.; Nychas, G.-J. E. Volatilomics for Food Quality and Authentication. *Curr. Opin. Food Sci.* **2019**, *28*, 88−95.

(4) Román, S.; Sánchez-Siles, L. M.; Siegrist, M. The Importance of Food Naturalness for Consumers: Results of a Systematic Review. *Trends Food Sci. Technol.* **2017**, *67*, 44−57.

(5) Petrescu, D. C.; Vermeir, I.; Petrescu-Mag, R. M. Consumer Understanding of Food Quality, Healthiness, and Environmental Impact: A Cross-National Perspective. *Int. J. Environ. Res. Public Health* **2020**, *17* (1), 169.

(6) Abou-el-karam, S.; Ratel, J.; Kondjoyan, N.; Truan, C.; Engel, E. Marker Discovery in Volatolomics Based on Systematic Alignment of GC-MS Signals: Application to Food Authentication. *Anal. Chim. Acta* **2017**, *991*, 58−67.

(7) Hatzakis, E. Nuclear Magnetic Resonance (NMR) Spectroscopy in Food Science: A Comprehensive Review. *Compr. Rev. Food Sci. Food Saf.* **2019**, *18* (1), 189−220.

(8) Bharti, S. K.; Roy, R. Quantitative 1H NMR Spectroscopy. *TrAC Trends Anal. Chem.* **2012**, *35*, 5−26.

(9) Akoka, S.; Barantin, L.; Trierweiler, M. Concentration Measurement by Proton NMR Using the ERETIC Method. *Anal. Chem.* **1999**, *71* (13), 2554−2557.

(10) Manual, B. *Eretic2 User's Guide: Preliminary*; Bruker Biospin 2012.

(11) Abraham, R. J.; Fisher, J.; Loftus, P. *Introduction to NMR Spectroscopy*; Wiley: Chichester, New York, 1988.

(12) Hyberts, S. G.; Robson, S. A.; Wagner, G. Exploring Signal-to-Noise Ratio and Sensitivity in Non-Uniformly Sampled Multi-Dimensional NMR Spectra. *J. Biomol. NMR* **2013**, *55* (2), 167−178.

(13) Emwas, A.-H.; Roy, R.; McKay, R. T.; Tenori, L.; Saccenti, E.; Gowda, G. A. N.; Raftery, D.; Alahmari, F.; Jaremko, L.; Jaremko, M.; Wishart, D. S. NMR Spectroscopy for Metabolomics Research. *Metabolites* **2019**, *9* (7), 123.

(14) Schwalbe, H. New 1.2 GHz NMR Spectrometers- New Horizons? *Angew. Chem., Int. Ed.* **2017**, *56* (35), 10252−10253.

(15) Hopson, R. E.; Peti, W. Microcoil NMR Spectroscopy: A Novel Tool for Biological High Throughput NMR Spectroscopy. In *Structural Proteomics*; Kobe, B.; Guss, M.; Huber, T., Eds.; Walker, J. M., Series Ed.; Methods in Molecular Biology; Humana Press: Totowa, NJ, 2008; Vol. *426*, pp 447−458. DOI: 10.1007/978-1-60327-058-8_30.

(16) Mulder, F. A. A.; Tenori, L.; Luchinat, C. Fast and Quantitative NMR Metabolite Analysis Afforded by a Paramagnetic Co-Solute. *Angew. Chem.* **2019**, *131* (43), 15427−15430.

(17) Bara-Estaún, A.; Harder, M. C.; Lyall, C. L.; Lowe, J. P.; Suturina, E.; Hintermair, U. Paramagnetic Relaxation Agents for Enhancing Temporal Resolution and Sensitivity in Multinuclear FlowNMR Spectroscopy. *Chem. − Eur. J.* **2023**, *29* (38), No. e202300215.

(18) Lolli, V.; Renes, E.; Caligiani, A.; de la Fuente, M. A.; Gómez-Cortés, P. Cyclopropane Fatty Acids as Quality Biomarkers of Cheeses from Ewes Fed Hay- and Silage-Based Diets. *J. Agric. Food Chem.* **2021**, *69* (33), 9654−9660.

(19) Caligiani, A.; Marseglia, A.; Palla, G. An Overview on the Presence of Cyclopropane Fatty Acids in Milk and Dairy Products. *J. Agric. Food Chem.* **2014**, *62* (31), 7828−7832.

(20) Marseglia, A.; Caligiani, A.; Comino, L.; Righi, F.; Quarantelli, A.; Palla, G. Cyclopropyl and $\omega$-Cyclohexyl Fatty Acids as Quality Markers of Cow Milk and Cheese. *Food Chem.* **2013**, *140* (4), 711−716.

(21) Lanza, I.; Lolli, V.; Segato, S.; Caligiani, A.; Contiero, B.; Lotto, A.; Galaverna, G.; Magrin, L.; Cozzi, G. Use of GC−MS and 1H NMR Low-Level Data Fusion as an Advanced and Comprehensive Metabolomic Approach to Discriminate Milk from Dairy Chains Based on Different Types of Forage. *Int. Dairy J.* **2021**, *123*, No. 105174.

(22) Lolli, V.; Marseglia, A.; Palla, G.; Zanardi, E.; Caligiani, A. Determination of Cyclopropane Fatty Acids in Food of Animal Origin by 1H NMR. *J. Anal. Methods Chem.* **2018**, *2018*, 8034042.

(23) Imperiale, S.; Kaneppele, E.; Morozova, K.; Fava, F.; Martini-Lösch, D.; Robatscher, P.; Peratoner, G.; Venir, E.; Eisenstecken, D.; Scampicchio, M. Authenticity of Hay Milk vs. Milk from Maize or Grass Silage by Lipid Analysis. *Foods* **2021**, *10* (12), 2926.

(24) Moore, B. S.; Floss, H. G. Biosynthesis of Cyclic Fatty Acids Containing Cyclopropyl-, Cyclopentyl-, Cyclohexyl-, and Cyclo-heptyl-Rings. In *Comprehensive Natural Products Chemistry*; Elsevier, 1999; pp 61−82. DOI: 10.1016/B978-0-08-091283-7.00002-3.

(25) Commission Regulation (EU) No 794/2011 of 8 August 2011 Approving Amendments to the Specification for a Name Entered in the Register of Protected Designations of Origin and Protected Geographical Indications (Parmigiano Reggiano (PDO)).

(26) Caligiani, A.; Nocetti, M.; Lolli, V.; Marseglia, A.; Palla, G. Development of a Quantitative GC−MS Method for the Detection of Cyclopropane Fatty Acids in Cheese as New Molecular Markers for Parmigiano Reggiano Authentication. *J. Agric. Food Chem.* **2016**, *64* (20), 4158−4164.

(27) Bahadoor, A.; Brinkmann, A.; Melanson, J. E. 13C-Satellite Decoupling Strategies for Improving Accuracy in Quantitative Nuclear Magnetic Resonance. *Anal. Chem.* **2021**, *93* (2), 851−858.

(28) Fujiwara, T.; Anai, T.; Kurihara, N.; Nagayama, K. Frequency-Switched Composite Pulses for Decoupling Carbon-13 Spins over ultrabroad Bandwidths. *J. Magn. Reson. A* **1993**, *104* (1), 103−105.

(29) Olson, D. L.; Peck, T. L.; Webb, A. G.; Magin, R. L.; Sweedler, J. V. High-Resolution Microcoil 1H-NMR for Mass-Limited, Nanoliter-Volume Samples. *Science* **1995**, *270* (5244), 1967−1970.

(30) Badilita, V.; Meier, R. C.; Spengler, N.; Wallrabe, U.; Utz, M.; Korvink, J. G. Microscale Nuclear Magnetic Resonance: A Tool for Soft Matter Research. *Soft Matter* **2012**, *8* (41), 10583.

(31) Lister, A. S. 7 - Validation of HPLC Methods in Pharmaceutical Analysis. In *Separation Science Technology*; Elsevier, 2005; Vol. 6, pp 191−217. DOI: 10.1016/S0149-6395(05)80051-0.

(32) Knothe, G. NMR Characterization of Dihydrosterculic Acid and Its Methyl Ester. *Lipids* **2006**, *41* (4), 393−396.

(33) Coote, P. W.; Robson, S. A.; Dubey, A.; Boeszoermenyi, A.; Zhao, M.; Wagner, G.; Arthanari, H. Optimal Control Theory Enables homonuclear Decoupling without Bloch-Siegert Shifts in NMR Spectroscopy. *Nat. Commun.* **2018**, *9* (1), 3014.

(34) Saito, N.; Komatsu, T.; Suematsu, T.; Miyamoto, T.; Ihara, T. Unique Usage of a Classical Selective Homodecoupling Sequence for High-Resolution Quantitative 1H NMR. *Anal. Chem.* **2020**, *92* (20), 13652−13655.

(35) Anklin, C.; Byrd, R. A. Combined Multi-band Decoupling in Biomolecular NMR Spectroscopy. *J. Biomol. NMR* **2021**, *75* (2−3), 89−95.

(36) Kupče, Ē. Applications of Adiabatic Pulses in Biomolecular Nuclear Magnetic Resonance. In *Methods in Enzymology*; Elsevier, 2002; Vol. *338*, pp 82−111. DOI: 10.1016/S0076-6879(02)38216-8.